



1 **Influence of Sea Surface Temperature on the Columnar Water**
2 **Vapor Content and Cloud Fraction, Based on Monthly-Averaged**
3 **MODIS Data at 1° by 1° Resolution**

4

5

Jung Eun Park and Taewoo Lee*

6

Mechanical and Aerospace Engineering, SEMTE

7

Arizona State University, Tempe, AZ, USA

8

9

10

11

12

13

14 *T.W. Lee, Corresponding author, attwl@asu.edu

15



16

17

18

19

20

21 **Abstract-** Satellite data on global sea surface temperature (SST), water vapor and
22 cloud fraction are analyzed to provide direct relationships on these parameters. Increase
23 in SST elevates the water vapor pressure at the surface following the Clausius-Clayperon
24 (exponential) form, and this effect persists to increase the columnar water vapor up to
25 SST of approximately 300 K, at the 1° by 1°, monthly-averaged scale. Beyond SST of 300
26 K, a steeper slope for the columnar water vapor is observed. A similar transitional
27 relationship is observed between cloud fraction (CF) and SST, except that a negative slope
28 is found up to SST of 300 K. Then, a reversal occurs at SST of approximately 300K where
29 CF increases quadratically as a function of SST. Parameterization of water vapor and CF
30 is provided as a function of SST for 1° by 1° spatial resolution and monthly-averaged time
31 scale.

32

33

34

35

36



37 1. INTRODUCTION

38 The Earth climate system is arguably the most important scientific and engineering
39 problem of our time, as it affects nearly all aspects of human existence and beyond. The
40 cloud fraction (CF) and sea surface temperature (SST) are two of the fundamental
41 parameters that affect the climate state. The cloud fraction is directly related to the
42 atmospheric albedo, while SST and its lateral gradients are the drivers of the advection
43 processes. The clouds are also attributed to trapping of the outgoing infrared radiation
44 (Perkins, 2010; Wu et al., 2019). Water vapor equilibrium is set at the sea surface
45 temperature, and convection of this vapor content leads to cloud fraction. Prior works
46 analyze the cloud fraction as a key climate feedback parameter (Cess et al., 1996; Ingram,
47 2010; Houghton, 1990; and Stocker et al., 2001). The atmospheric optical depth and
48 cloud fraction are close correlated (Engstrom and Ekman, 2010; Gryspeerdt et. al, 2014).
49 For these reasons, inter-relationships between the basic climate variables such as SST,
50 water vapor (WV), and cloud fractions are important in understanding of the Earth
51 climate system. Thermodynamically, Clausius-Claperyon equation specifies the liquid-
52 vapor equilibrium based on water temperature, e.g. SST. However, observational data for
53 the columnar water vapor as a function of SST tend to deviate from this relationship, and
54 modified constants are used depending on spatial locations (Zhang and Qiu, 2008;
55 Stephens, 1990; Kanemaru and Masunaga, 2013). Stephens (1990), for example,
56 examined the global relationships between SST and precipitable water vapor at the same
57 coordinate, and showed that the Clausius-Claperyon form is applicable for $SST > 15\text{ }^{\circ}\text{C}$
58 with less than 20% deviation potentially arising from large-scale flow effects. Constants
59 in the SST-WV relationship have been obtained through least-square fit with passive
60 microwave radiometry data (Stephens, 1990). Waliser (1996) investigated the SST-
61 atmosphere interaction by examining thermodynamic and convection dynamic variables,
62 suggesting that there is a feedback mechanism to suppress locally high SST. Ramanathan
63 and Collins (1991) found that the net greenhouse effect increased as a function of the sea
64 surface temperature, during 1987 El Nino event. However, this was offset by cirrus cloud
65 reflection of incoming solar radiation at $SST > 300\text{ K}$. Kanemaru and Masunaga (2013)
66 analyzed the surface moisture and vertical gradients, and found different moisture
67 structure depending on latitude regions (e.g. sub-tropical, tropical). Yu and Weller
68 (2007) found that the surface latent heat flux bears a great similarity to that of SST,
69 leading to increased moisture-holding capacity of the atmosphere in line with SST.

70



71 Analyses and computations of the Earth climate system typically include detailed
72 spatio-temporal developments of climate variables including turbulent convection
73 (Larson and Hartmann, 2003; Randall et al., 2007). For example, in a typical global
74 circulation model (GCM) the ocean convection currents set the surface boundary
75 conditions. Then, phase-equilibrium models need to be applied to compute the
76 atmospheric water vapor and cloud formation leading to varying results which often are
77 model-dependent (Cess et al., 1990, Randall et al., 2007; Yu et al., 2004). These GCM
78 models are useful in assessing the interaction of local and surrounding environmental
79 variables. However, detailed and accurate simulations of entire global circulation are
80 intrinsically difficult and time-consuming. In addition, modeling of cloud formation at
81 different altitudes adds a significant level of complexity in GCM simulations due to non-
82 linear thermodynamics and multiple parameters in a typical cloud fraction model (Hu,
83 1997; Xu et al., 2010). Possibly for this reason, there have not been as much reported
84 findings on relationship between SST with CF, compared to SST-WV analyses. Nair and
85 Rajeev (2014) have considered SST and dynamical effects on vertical cloud distributions.
86 Similar to WV, warmer SST is associated with increased upward convection (and
87 turbulence), which affects the vertical distribution (Nair and Rajeev, 2014). Similar
88 latitude (regional) differences are also expected.

89 Thus, the current approach is to first analyze the monthly averaged data, and seek
90 fundamental first-order relationships between SST, WV and also CF, leading to some
91 understanding of the global thermodynamic processes. A pre-cursor attempt was
92 somewhat inconclusive (Lee and Park, 2022), and in the current work the analysis has
93 been revised and re-examined to reveal some insight and succinct relationships for the
94 fundamental climate variables, in particular directly between sea surface temperature and
95 cloud fraction.

96

97 **2. DATA ANALYSES**

98 For understanding and predicting the Earth climate system, satellite-based,
99 higher-level processed data sets are readily available including SST, WV and CF at various
100 spatial and temporal resolutions. These data sets are often used during the key necessary
101 step of validating and calibrating the computational models of the Earth climate system
102 (Jiang et al., 2012). At a basic level, these data can be analyzed and examined from
103 various perspectives (e.g., thermodynamic) to gain understanding of the important
104 forcing functions, such as the relationship between the SST to columnar water vapor,
105 cloud fraction, and others (Lee and Park, 2022). In this work, SST, WV and CF provided



106 in the MODIS data products are used for analyses (Lee and Park, 2026). Detailed
107 descriptions of the data and processing methods are discussed by various authors of the
108 MODIS data set (<https://modis.gsfc.nasa.gov/data/>). We use the 1° by 1° resolution,
109 monthly-averaged data in this work, for the time span of January 2000 to March of 2017.
110 The unit for the columnar water vapor (WV) is in cm, which is the standard definition for
111 the height of the water if the entire columnar water vapor condensed in that cell. These
112 data are plotted in scattergrams (Figs. 1-5), while least-square fit regressions are
113 attempted for quantitative correlations. Due to the large range of spatial and temporal
114 scales, a fair amount of scatter exists in the plots, which is also discussed.

115

116 **3. RESULTS AND DISCUSSION**

117 Satellite data on global sea surface temperature (SST), water vapor and cloud
118 fraction are analyzed, and inter-dependence of these parameters are attempted. As is well
119 known, SST produces the water vapor in the atmosphere through the thermodynamics of
120 saturation pressure and temperature. This is evident in SST vs. WV scattergrams (Figure
121 1), where a Clausius-Claperyon (CC) form of exponential dependence on SST is observed
122 up to SST of approximately 300 K. With minor adjustments in the CC form, the columnar
123 WV content can be tracked up to this transition point ($T_c \sim 300$ K). Beyond that, the slope
124 increases substantially, above the typical CC-form. Other researchers have modified the
125 constants in the CC equation to span the entire SST range (Zhang and Qiu, 2008;
126 Stephens, 1990; Kanemaru and Masunaga, 2013). However, due to the above-noted
127 transition near T_c of 300 K, SST-WV can be considered separately in two segments, SST
128 $< T_c$ and SST $> T_c$. The CC exponential form be effectively used up to T_c , but an alternate
129 expression needs to be adopted to correlate WV with SST beyond that point. This
130 transition is present in all of the data spanning 2000 to 2017 (a small sub-set is shown in
131 Fig. 1), with minor month-to-month variations. During some months, the data are
132 bifurcated for SST < 285 K, with upper branch exhibiting higher WV than the lower CC
133 branch. These months are also associated with larger scatter in the data, in Figure 1.

134

135 We note that the CC-form equations are based on the sea-surface temperature,
136 while the measured water vapor is for the entire columnar height above that location.
137 Therefore, vertical convection can influence the WV (Kanemaru and Masunaga, 2013).
138 In addition, low/high SST is mostly associated with high/low latitudes, and the two
139 distinct behavior can arise from latitude effects. Other authors have also found such
140 differences in SST-WV in subtropical and tropical regions (Kanemaru and Masunaga,



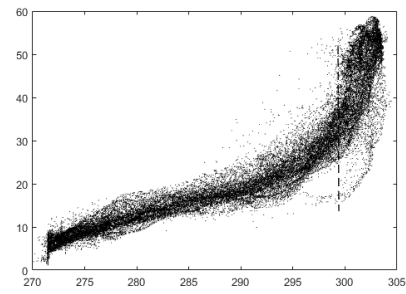
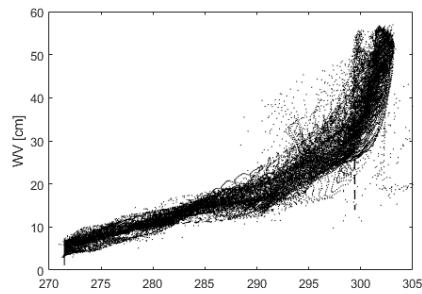
141 2013; Stephens, 1990). At low to moderate temperatures (SST < 300 K), the water vapor
142 content is dominated by the amount near the sea surface. At higher temperature (SST >
143 300 K), increased evaporation and SST leads to appreciable upward convection. Data
144 plotted in Figure 1 indicate that the water vapor content is “over-saturated”, higher than
145 the water vapor pressure at the corresponding SST, SST of of approximately 300 K. This
146 observation for SST > 300K is replicated for all of the monthly data set (Figure 1 is a
147 representative subset of the entire data set). This bi-fold behavior appears to also have an
148 effect on the cloud fraction, as discussed later. Dynamical effects can evidently influence
149 SST-WV relations. As noted above Stephens (1990) also found that the Clausius-
150 Claperyon form is applicable for SST > 15 C° with less than 20% deviation potentially
151 arising from large-scale flow effects. The scatter in the data increases progressively from
152 SST ~ 275 K to 300 K. Stephens (1990) quantified the potential effects of large-scale flows
153 to approximately 20%, and the amount of scatter in the data in Fig. 1 appears to reflect
154 this convection variability.

155

156 A similar transition is observed in the SST vs. CF (cloud fraction) scattergram (Fig.
157 2). The transition to a different slope occurs at about the same SST (~300 K). We observe
158 small month-to-month variations in this transition point of up to SST of +/- 2 K. For CF,
159 the transition is more dramatic as the slope is completely reversed: CF *decreases* with
160 respect to SST up to T_c , then steeply *increases* beyond it. The physical mechanism for this
161 reversal and increase in CF above the threshold temperature (T_c) may again be attributed
162 to the increased upward convection at high SST, distributing the water vapor to higher
163 altitude resulting in more vapor available for condensation and cloud formation. We
164 again note that the SST-WV correlation in Figure 1 is with respect to SST and thus
165 representative of water vapor present near the sea surface. Any upward mobility in water
166 vapor will increase the availability of WV at higher altitude/lower temperature, and
167 condensation can occur leading to cloud formation. The decrease in CF with increasing
168 SST below SST ~ 300K is apparently due to increasing saturation pressure (with SST) so
169 that atmosphere is able to hold water vapor prior to condensation (cloud formation).
170 These trends are consistently observed in all of the months in the data set, as will be shown
171 later. There is a larger amount of scatter in the data, probably due to complex, multiple
172 factors that can influence cloud formation (Nair and Rajeev, 2014). From the global
173 thermodynamic perspective, the steep positive slope in CF with SST (SST > 300 K)
174 provides a negative forcing of the global warming, as CF reflects a large portion of the
175 incoming solar radiation.

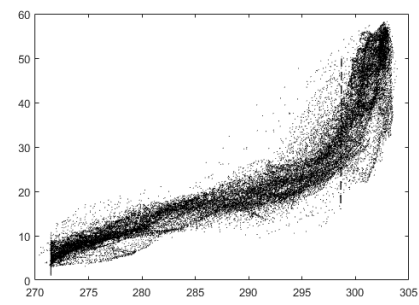
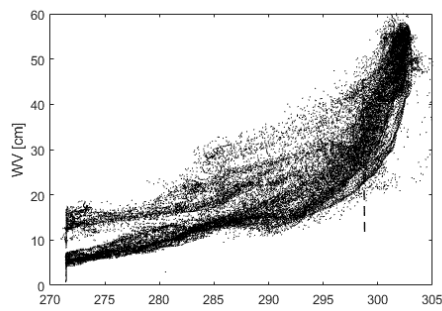


176

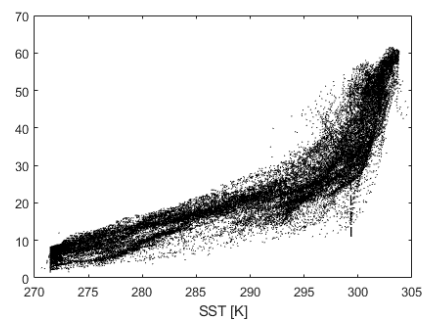
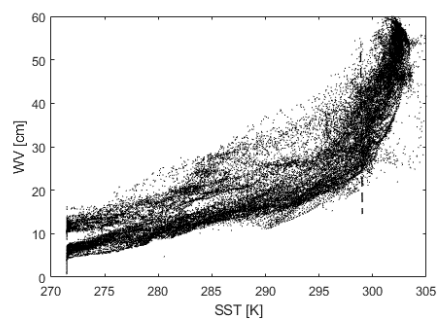


177

178



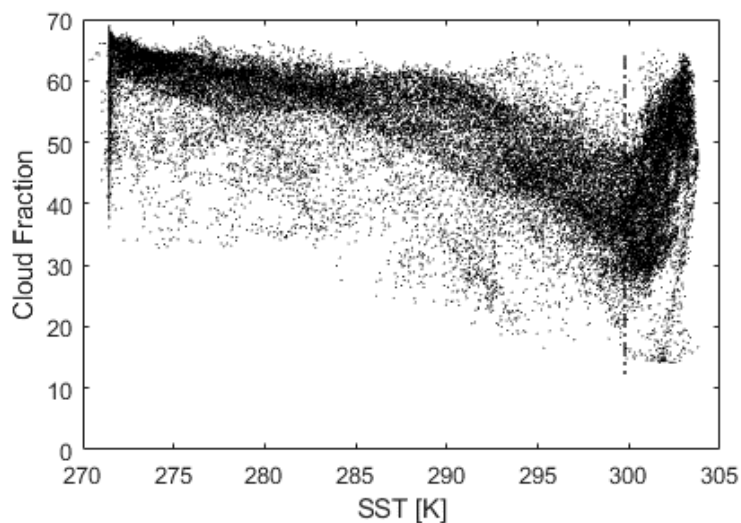
179



180

181

182 **Figure 1. Water vapor (WV) vs. SST scattergram for various months (from**
183 **top left: October, 2000; April, 2003; August, 2007; April, 2013; December,**
184 **2015; and December 2019).**



185

186 **Figure 2. Cloud fraction (CF) vs. SST scattergram for May, 2007.**

187

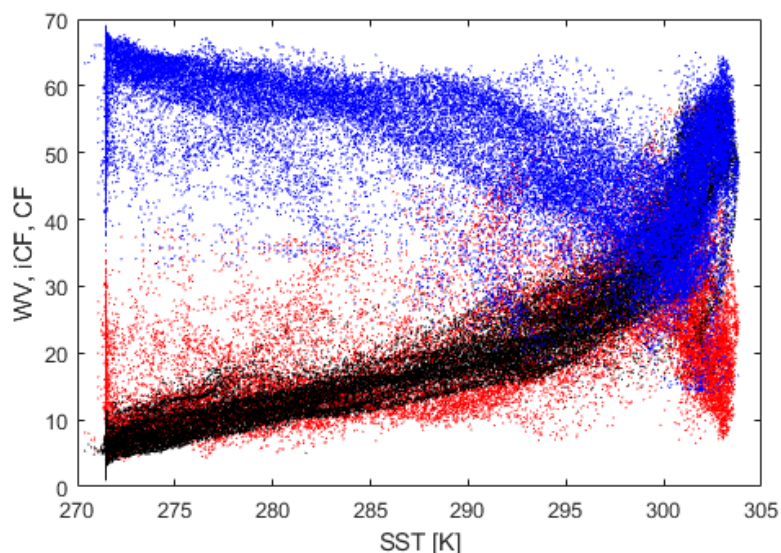
188 Above trends can be further examined by plotting shifted and/or inverted SST-CF
189 data on top of the SST-WV (red), as shown in Figure 3. First, we use SST-WV correlational
190 data (the same plots as in Figures 1 and 2, except plotted in red) as the reference. Then,
191 we upward-shift the SST-CF data (black) on top of this reference data set, which results
192 in overlap of WV and CF as a function of SST for $SST > T_c$ (~300K) in Figure 3. This
193 explains the over-saturation (large WV) at these SST's directly produces large cloud
194 fraction (CF). Upward shifting is simply to match the vertical axis scale for WV and CF.
195 Inversion of the same SST-CF data (blue) matches the SST-WV curve (red) for $SST < T_c$
196 region. WV increased with SST, while CF decreased when $SST < T_c$, so that inverting CF
197 results in an overlap for $SST < T_c$ in Figure 3. This simply means that below $SST < T_c$ the
198 increase in saturation pressure withholds cloud formation in the atmosphere. Thus, the
199 global data set strongly indicates that SST can be used as a single determinant for both
200 WV and CF at 1° by 1° resolution, and with monthly time-averaging. The amount of
201 scatter in the data is intrinsic at these scales, but the observed trends are consistent and
202 clear. Considering that other models of cloud fraction are quite complex and incur
203 deviations depending on the local conditions, the current correlational data for SST, WV
204 and CF point to consistent and logical thermodynamic trends. Similar to SST-WV data,
205 these trends are observed for all of the observed months during 2000 to 2017, as shown
206 in Figure 4. However, there is an increasing data scatter as SST increases in the SST-CF



207 plots. As noted above, cloud formation processes are quite complex starting from surface
208 level moisture corresponding to SST, but involving upward and lateral convection, and
209 altitude-dependent condensation (Nair and Rajeev, 2013). Nonetheless, as a first-order
210 estimation of CF directly parameterized as a function of SST, current trends indicate a
211 distinct two-fold CF behavior, below and above SST of approximately 300 K. In
212 particular, a complete reversal in CF slope at high SST suggests that there may be an
213 alleviating factor at this SST range.

214

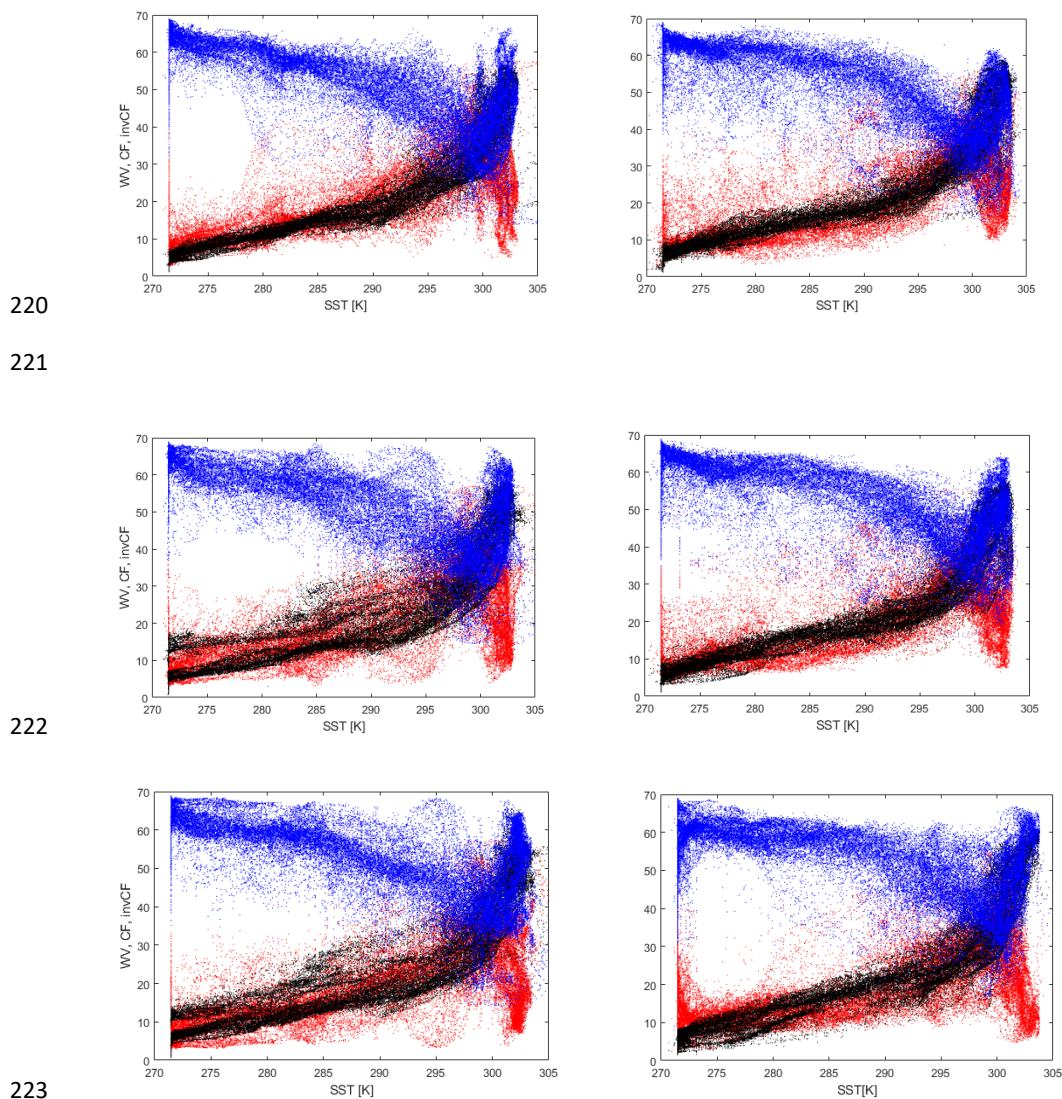
215



216

217 **Figure 3. Relationship between WV (black), CF (blue) and inverted CF (red)**
218 **vs. SST (May. 2007).**

219



220

221

222

223

224 **Figure 4. WV (black), CF (blue) and inverted CF (red) vs. SST scattergram**
225 **for various months (from top left: October, 2000; April, 2003; August,**
226 **2007; April, 2013; December, 2015; and December 2019).**

227

228

229



230 In summary, when plotted as a function of SST, the cloud fraction is correlated
231 with SST for $SST > T_c$ due to over-saturation, but is anti-correlated when $SST < T_c$ due to
232 increasing saturation pressure. In spite of the fairly large scatter in the data, a set of
233 quantitative correlations between SST [K] and WV [cm] or CF, as a first-order estimation,
234 is attempted as follows:

235

236 $WVa = 17.77 \times 10^7 \exp(0.068 * (SST - 661.15)),$ for $SST < T_c$ (1a)

237

238 $WVb = -6.75 + 0.0215(SST - 278.65)^2,$ for $SST > T_c$ (1b)

239

240

241 $CFa = 1.03125 - 2.22 \times 10^7 * \exp(0.068 * (SST - 561.15)),$ for $SST < T_c$ (2a)

242

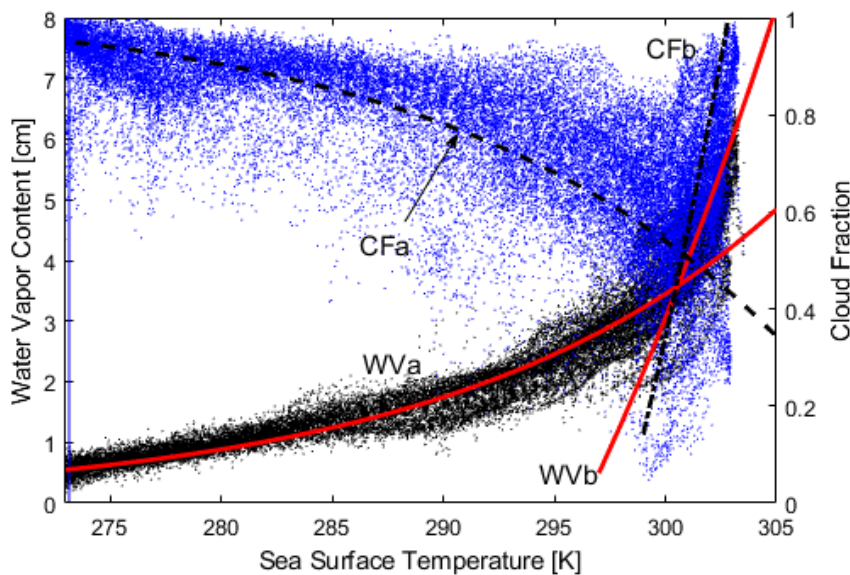
243

244 $CFb = -1 + 0.008125(SST - 287.15)^2,$ for $SST > T_c$ (2b)

245

246

247 T_c is taken as 300 K. The functionality of the correlation is demonstrated in Figure 5. The
248 cloud fraction is an exact inversion of the water vapor trace for $SST < T_c$, and follows
249 Clausius-Claperyon type of function (exponential, Eqs. 1a and 2a). However, for $SST > T_c$
250 the steep increase in both WV and CF is better traced by quadratic curves (Eqs. 1b and
251 2b). As shown in Figure 4, these traces are replicated for most of the months in the data
252 set. There is a fair amount of scatter in the data relative to the above correlations. At SST
253 $= 285$ K, the variances are $+25/-9\%$ for WVa and $+6/-5\%$ for CFa relative to the correlation
254 functions (Ea. 1a and 2a). At $SST = 302$ K, the variances $+11/-7\%$ for WVb and $+12/-20\%$
255 for CFb , again relative to the correlations (Eqs. 1b and 2b). Stephens (1990) attributed
256 approximately 20% to the large-scale flow effects, and the data variances are at about this
257 level in the current observational data. Considerations of other variables have two facets
258 of incorporating convection effects but also complicating the modeling process.
259 Therefore, at this point we present the above correlations as a first-order modeling and
260 analysis tool, while acknowledging the data variance to be considered in subsequent
261 studies.



262

263 **Figure 5. Correlational relationships (Eqs. 1 and 2) for WV [cm] and CF, as**
264 **a function of SST.**

265

266

267 **4. CONCLUDING REMARKS**

268 Water vapor content and cloud fraction both exhibit direct correlatability with the
269 sea surface temperature, when averaged over 1° by 1° area on a monthly basis. A
270 transition occurs at SST ~ 300 K, where the water vapor content sharply increases. Cloud
271 fraction decreases with SST up to this transitional SST of 300 K. Then, it reverts to an
272 increasing function of SST. These trends are quite repeatable over a fairly long time
273 period, from 2000 to 2017, and parameterized as a function of SST (Eqs. 1 and 2). Thus,
274 SST can be used as a primary determinant for the resulting atmospheric variables (WF
275 and CF) at these spatial and temporal scales. There is a fair amount of scatter in the data
276 (5 to 25%), relative to the mean relationships developed in this work, which is attributable
277 to secondary effects such as convection and other local variations. Incorporation of these
278 effects, using data sets at finer temporal and spatial scales, can be considered in future
279 work.

280



281 **5. Data Availability**

282 The data used in this work is available at <https://doi.org/10.5281/zenodo.19389633> (Lee
283 and Park, 2026).

284

285 **REFERENCES**

286

287 Arkin, P.A., The relationship between fraction coverage of high cloud and rainfall
288 accumulations during GAT over the B-scale array, *Monthly Weather Review*, Vol. 107,
289 pp. 1382-1387, 1979.

290

291 Cess, R. D., Potter, G. L., Blanchet, J. P., Boer, G. J., Del Genio, A. D., Deque, M., ... &
292 Zhang, M. H., Intercomparison and interpretation of climate feedback processes in 19
293 atmospheric general circulation models. *Journal of Geophysical Research:*
294 *Atmospheres*, 95(D10), 16601-16615, 1990.

295

296 Cess, R.D., and co-authors, Cloud feedback in atmospheric general circulate models: An
297 update., *Journal of Geophysical Research*, Vol. 101, pp. 12791-12794, 1996.

298

299 Engström, A. and Ekman, A.M.L., Impact of meteorological factors on the correlation
300 between aerosol optical depth and cloud fraction, *Geophysical Research Letters*, Vol.
301 37, L18814, doi:10.1029/2010GL044361, 2010

302

303 Gaffens, D.J., Elliott, W.P., and Robock, A., Relationship between tropospheric water
304 vapor and surface temperature as observed by radiosondes, *Geophysical Research*
305 *Letters*, Vol. 19, 18. 1992.

306

307 Gryspeerdt, E., P. Stier, and B. S. Grandey, Cloud fraction mediates the aerosol optical
308 depth-cloud top height relationship, *Geophysical Research Letters*, Vol. 41, pp. 3622–
309 3627, 2014.



310

311 Houghton, J.G., Jenkins, G.J., and Ephraums, Eds., *Climate Change: The IPCC*
312 *Scientific Assessment*, Cambridge University Press, 1990.

313

314 Hu, Q., A cumulus parameterization based on a cloud model of intermittently rising
315 thermals, *Journal of Atmospheric Sciences*, 54, 18, 2292-2307, 1997.

316

317 Jiang, J.H., Su, H., Zhai, C., Perun, V.S., Del Genio, A., Evaluation of cloud and water
318 vapor simulations in CMIP5 climate models Using NASA “A-Train” satellite
319 observations, *Journal of Geophysical Research: Atmospheres*, Vol. 117(14), pp.
320 D14105, 2012.

321

322 Kanemaru, K. and Masunaga, H., A satellite study of the relationship between sea
323 surface temperature and column water vapor over tropical and subtropical oceans,
324 *Journal of Climate*, Vol. 26, pp. 4204-4218, 2013.

325

326 Kennedy, A.D., Dong, X., Xi, B., Xie, S., Zhang, Y., and Chen, J., A Comparison of
327 MERRA and NARR Re-analyses with the DOE ARM SGP Data, *Journal of Climate*, Vol.
328 24, pp. 4541-4557, 2011.

329

330 Lee, T.-W. and Park, J.E., Thermodynamic correlations between the sea surface
331 temperature, water vapor content, and cloud fraction, using MODIS data. *Theoretical*
332 *and Applied Climatology*, 150, 1699–1706 (2022).

333

334 Lee, T.-W. and Park, J.E., Monthly averages of water vapor, cloud fraction and SST
335 (2026), <https://doi.org/10.5281/zenodo.19389633>

336

337 Nair, A.K.M. and Rajeev, K, Multiyear CloudSat and CALIPSO Observations of the
338 Dependence of Cloud Vertical Distribution on Sea Surface Temperature and



- 339 Tropospheric Dynamics, *Nature Climate Change*,
340 <https://doi.org/10.1038/nclimate1026>, 2010.
- 341
- 342 Price, J. D., A study of probability distributions of boundary-layer humidity and
343 associated errors in parametrized cloud-fraction, *Quarterly Journal of the Royal*
344 *Meteorological Society*, Vol. 127, No. 573, pp. 739-758, 2001.
- 345
- 346 Qian, Y., Long, C.N., Wang, H., Comstock, J.M., McFarlane, S.A., and Xie, S., Evaluation
347 of cloud fraction and its radiative effect simulated by IPCC AR4 global models against
348 ARM surface observations, *Atmospheric Chemistry and Physics*, Vol. 12, pp. 1785–
349 1810, 2012.
- 350
- 351 Ramanathan, V., Collins, W. Thermodynamic regulation of ocean warming by cirrus
352 clouds deduced from observations of the 1987 El Niño. *Nature* 351, 27–32, 1991.
- 353
- 354 Randall, David A., et al. "Climate models and their evaluation." *Climate change 2007:*
355 *The physical science basis. Contribution of Working Group I to the Fourth Assessment*
356 *Report of the IPCC (FAR)*. Cambridge University Press, 2007. 589-662.
- 357
- 358 Stephens, G.L., On the relationship between water vapor over the oceans and sea surface
359 temperature, *J. Climate*, Vol. 3, pp. 634-645, 1991.
- 360
- 361 Stocker, T.F., and co-authors, Climate processes, *Climate Change 2001: The scientific*
362 *basis (J.T. Houghton et al., Eds)*, Cambridge University Press, 2001.
- 363
- 364 Wu, K., Li, J., Cole, J., Huang, X., von Salzen, K. and Zhang, F., Accounting for Several
365 Infrared Radiation Processes in Climate Models, *Journal of Climate*, 32, 4601-4620
366 (2019).
- 367



368 Xu, K-M, Cheng, A., and Zhang, M., Cloud-Resolving Simulation of Low-Cloud
369 Feedback to an Increase in Sea Surface Temperature, *Journal of Atmospheric Sciences*,
370 67, 3, 730-748, 2010.

371

372 Yongqiang, Y., Xuehong, Z. and Yufu, G., Global coupled ocean-atmosphere general
373 circulation models in LASG/IAP., *Advances in Atmospheric Science*, 21, 444–455,
374 2004.

375

376 Zhang, C. and Qiu, F., Empirical relationship between sea surface temperature and
377 water vapor: improvement of the physical model with remote sensing derived data,
378 *Journal of Oceanography*, Vol. 64, pp. 163-170, 2008.